Research Square

Preprints are preliminary reports that have not undergone peer review.
They should not be considered conclusive, used to inform clinical practice,
or referenced by the media as validated information.

Rapid tetracycline degradation by a hydroxylamine/chloride- enhanced zero-valent copper/peroxydisulfate system under near- neutral conditions

Quan Yu
Hunan University of Science and Technology
Renjian Deng
waterdrj@hnust.edu.cn

Hunan University of Science and Technology
Xin Liu
University of South China
Baolin Hou
Hunan University of Science and Technology
Saijun Zhou
Hunan University of Science and Technology
Chuang Wang
Hunan University of Science and Technology
Xifeng Wang
Hunan University of Science and Technology
Bozhi Ren
Hunan University of Science and Technology
Sihui Li
Xiangtan Zhonghuan Water Affairs Co. Ltd
Wei Huang
Xiangtan Zhonghuan Water Affairs Co. Ltd

Research Article

Keywords: Tetracycline, Peroxydisulfate, Zero-valent copper, Hydroxylamine, Chloride, Advanced oxidation

Posted Date: November 2nd, 2026

DOI: https://doi.org/10.21203/rs.3.rs-11376448/v1

License: This work is licensed under a Creative Commons Attribution 4.0 International License.
Read Full License

Additional Declarations: No competing interests reported.

Abstract

Limited copper(I) availability constrains peroxydisulfate (PDS) activation by zero-valent copper (Cu^0). This study evaluates the combined effects of hydroxylamine (HA) and chloride by comparing matched Cu^0/PDS control systems and relating tetracycline (TC) removal to measured copper(I) concentrations and PDS consumption. At an initial pH of 5.0, TC removal after 10 min was 11.1% without either additive, 63.8% with HA, 23.8% with chloride and 86.2% with both; the combined-system apparent rate constant was 0.2119 min^{-1}. PDS consumption was 6%, 34%, 13% and 54%, respectively. These concurrent trends are consistent with complementary HA-assisted copper(I) regeneration and chloride-mediated stabilization, although they do not directly resolve individual copper(I) complexes or quantify an interaction between the additives. Electron paramagnetic resonance spectroscopy and quenching tests support radical involvement and possible reactive chlorine participation, without establishing copper(III) as the dominant oxidant. TC removal was 68.6% at initial pH 7.0, 77.1% in tap water and 67.7% in surface water. Total organic carbon removal was only 5.7% after 10 min, indicating limited mineralization. Alkaline precipitation and filtration reduced total dissolved copper from 7.16 to 0.673 mg/L. The study links combined-additive enhancement to copper(I) availability and oxidant consumption while identifying mineralization and copper management as limitations requiring further evaluation.

1. Introduction

The continuous discharge of antibiotic contaminants into aquatic environments has become a challenge in emerging pollutant treatment (Y. Li et al., 2024; X. Yang et al., 2024; X. Zhang et al., 2024; X. Zhou et al., 2024). Among them, tetracycline (TC) is difficult to remove efficiently by conventional wastewater treatment processes because of its extensive use, stable chemical structure and poor biodegradability. As a result, TC can persist in water bodies and undergo transport and transformation (Z. Li et al., 2019; Niu et al., 2024; Y. Yang et al., 2023; H. Zhang et al., 2024; X. Zhang et al., 2024; P. Zhou et al., 2018). More importantly, long-term exposure to TC may induce the proliferation of antibiotic-resistant bacteria and antibiotic resistance genes, thereby posing potential risks to aquatic ecosystems and human health (Y. Li et al., 2024; X. Zhang et al., 2024; X. Zhou et al., 2024). Therefore, developing efficient, stable and environmentally feasible technologies for TC removal is needed for water pollution control (He et al., 2023; Niu et al., 2024; Shi et al., 2025; Y. Yang et al., 2023; H. Zhang et al., 2024; P. Zhou et al., 2018).

Advanced oxidation processes (AOPs), which generate highly reactive oxidizing species in situ, have shown strong potential for the removal of refractory organic pollutants from antibiotic-containing wastewater (Ding et al., 2022; Y. Li et al., 2024; Oyekunle et al., 2021; X. Zhou et al., 2024). Among the available oxidants, peroxydisulfate (PDS, $S_2O_8^{2-}$) has attracted increasing attention because of its high oxidation capacity, good chemical stability, convenient storage and transportation, and broad applicability (Ding et al., 2022; Huang et al., 2024; Y. Li et al., 2024; P. Zhou et al., 2018). Once activated, PDS can generate sulfate radicals ($SO_4^{\bullet-}$) and hydroxyl radicals (•OH), while its reaction pathways can also involve non-radical or other reactive species depending on the activator and water matrix (Bai et al., 2026; Y. Li et al., 2024; Z. Li et al., 2019; L. Wang et al., 2025; Weng et al., 2022; P. Zhou et al., 2018).

Current research therefore focuses on developing efficient, low-energy and controllable PDS activation strategies, particularly those based on transition-metal-mediated redox cycles. However, the practical performance of these systems can still be limited by inefficient oxidant utilization, rapid depletion or transformation of the active metal species, and insufficient stability under near-neutral conditions (Ding et al., 2022; Y. Li et al., 2024; L. Wang et al., 2025; Weng et al., 2022; X. Zhou et al., 2021). Further clarification of the metal redox process and the roles of coexisting ions or additives is thus needed to develop more efficient and adaptable PDS-based oxidation systems.

Among transition-metal activators, iron-based catalysts have been widely studied because of their abundance, relatively low toxicity, and diverse catalytic structures. However, their performance depends strongly on catalyst composition, Fe speciation, support structure, and reaction conditions; acidic operation, surface passivation, or sludge accumulation may occur in traditional homogeneous Fenton systems or certain iron-based configurations, whereas many heterogeneous iron catalysts can operate over a broader pH range and reduce sludge formation through catalyst immobilization (Kaur et al., 2023; Liang et al., 2023; Shi et al., 2025; X. Zhou et al., 2024). In the present study, copper-based catalysts were selected because they can maintain favorable activation capability and reaction adaptability under neutral or weakly acidic conditions (Ding et al., 2022; Du et al., 2017; Z. Li et al., 2019; T. Liu et al., 2022; Zhong et al., 2020). In particular, zero-valent copper (Cu^0) can continuously release Cu^+ through self-corrosion or reaction with PDS, and the generated Cu^+ can further activate PDS to produce reactive oxidizing species. However, Cu^+ readily undergoes disproportionation or is oxidized by dissolved oxygen to Cu^{2+}, resulting in its rapid depletion. This insufficient Cu^+ availability remains a key bottleneck limiting the efficiency of Cu^0/PDS systems (Y. Chen et al., 2025; Z. Li et al., 2019; Xu, Feng, et al., 2025; Xu, Li, et al., 2025; X. Zhou et al., 2021). Therefore, how to stabilize Cu^+ and maintain its continuous supply through external additives or material structural design has become a core scientific issue for enhancing the performance of copper-based activation systems. Previous studies have shown that hydroxylamine (HA) can accelerate the reduction of Cu^{2+} to Cu^+ and promote Cu^0 corrosion, thereby strengthening the Cu^{2+}/Cu^+ redox cycle and sustaining oxidant activation in Cu^0-based systems (Chi et al., 2019; Dong et al., 2025; J. Wang et al., 2022; Xu, Feng, et al., 2025; H. Zhang et al., 2024). From the perspective of copper coordination chemistry, chloride ion (Cl^-), a ubiquitous anion in aquatic environments, can coordinate with Cu^+ to form relatively stable $[CuCl_x]^{(1-x)}$ complexes, which suppress Cu^+ disproportionation and its oxidation by dissolved oxygen, thereby improving the persistence and utilization efficiency of Cu^+ (B. Li et al., 2024; X. Liu et al., 2023; Oyekunle et al., 2021; Xu, Li, et al., 2025; Xu et al., 2023). In addition, Cl^- has been reported to promote the comproportionation between Cu^0 and Cu^{2+} to continuously replenish Cu^+, and to participate in the conversion of sulfate and hydroxyl radicals into reactive chlorine species during PDS activation (X. Liu et al., 2023; Oyekunle et al., 2021; Xu, Li, et al., 2025; Xu et al., 2023).

Previous studies have examined HA-enhanced Cu⁰/persulfate oxidation (Xu, Feng, et al., 2025) and chloride-enhanced activation of peroxysulfate by Cu⁰ (Xu, Li, et al., 2025). HA-assisted Cu⁰ activation has

also been reported for peroxymonosulfate (Chi et al., 2019). Combined HA/chloride approaches have been investigated in Cu^0/H_2O_2 oxidation of TC (X. Liu, Yu, et al., 2025) and in Cu^0-based acetaminophen degradation (X. Liu, Xin, et al., 2025). These studies establish the relevance of the individual additives and of their combination in related copper-based oxidation processes. For the present Cu^0/PDS system, the question is how the combined-additive response relates to Cu^+ availability and PDS consumption under matched conditions, and what treatment limitations remain. Here, comparisons among the baseline, HA-only, chloride-only and combined-additive Cu^0/PDS systems are considered alongside Cu^+ concentration and PDS consumption measurements. EPR and quenching tests provide complementary evidence on reactive species, while initial-pH and water-matrix experiments assess the conditions under which the removal response is retained. The contribution is an integrated evaluation of the combined-additive response and its proposed copper-cycling explanation, with TC disappearance assessed separately from mineralization and dissolved copper management.

This study aimed to (1) compare TC removal and degradation kinetics in matched Cu^0/PDS systems with HA, chloride, both additives or neither, including a control without PDS; (2) relate these comparisons to Cu^+ concentration, PDS consumption and HA transformation measurements, and use reactive species tests to assess a proposed explanation based on complementary Cu^+ regeneration and stabilization; and (3) examine initial-pH and water-matrix effects, copper reuse, mineralization and dissolved copper removal. The analysis distinguishes measured removal and oxidant-consumption responses from mechanistic interpretation and evaluates the limitations relevant to further water-treatment studies.

2. Materials and methods

2.1. Materials

Copper powder (Cu^0, ≥ 99.9% metals basis, ≤ 0.044 mm), hydroxylamine sulfate ($[(NH_2OH)_2{\cdot}H_2SO_4]$, AR, ≥ 99%), sodium periodate ($NaIO_4$, CP, ≥ 98%), neocuproine ($C_{14}H_{12}N_2$, ≥ 98%), tetracycline ($C_{22}H_{24}N_2O_8$, ≥ 96%), and potassium peroxydisulfate ($K_2S_2O_8$, > 99%) were purchased from Aladdin Reagent Co., Ltd. (Shanghai, China). Sodium hydroxide (NaOH, 96%), sulfuric acid (H_2SO_4, 95–98%), sodium thiosulfate ($Na_2S_2O_3$, 99%), and sodium chloride (NaCl, 99.8%) were obtained from Sinopharm Group Chemical Reagent Co., Ltd. (Shanghai, China). All reagents were used as received without further purification, and all stock solutions were freshly prepared with ultrapure water before use.

2.2. Experimental procedure

TC degradation experiments were conducted in 250 mL conical flasks under magnetic stirring at a fixed stirring speed of 600 rpm. All experiments were performed at 25 ± 1°C. Before each experiment, stock solutions of TC, HA, Cl^- and PDS were freshly prepared with ultrapure water. The initial pH of the reaction solution was adjusted to the desired value using NaOH or H_2SO_4 solution before the reaction. For a typical Cu^0/PDS/HA/Cl^- system, predetermined concentrations of TC, Cl^-, HA and PDS were sequentially added into the reactor and thoroughly mixed to obtain a homogeneous reaction solution. Subsequently, a

certain dosage of Cu^0 was added to initiate the reaction, and the moment of Cu^0 addition was defined as the initial reaction time. Unless otherwise specified, the standard reaction conditions were as follows: $[TC]_0$ = 5 mg/L, $[Cu^0]_0$ = 0.05 g/L, $[HA]_0$ = 0.3 mmol/L, $[PDS]_0$ = 0.1 mmol/L, $[Cl^-]_0$ = 3 mmol/L, and pH_0 = 5.0 ± 0.1. At predetermined time intervals, 2.5 mL aliquots were withdrawn from the reaction suspension using a pipette and immediately quenched with 0.5 mL of 5 mmol/L sodium thiosulfate solution to remove residual oxidants and terminate further oxidation. The quenched samples were filtered through 0.45 μm membrane filters to remove suspended Cu^0 particles and then used for subsequent analysis. The residual TC concentration was determined by high-performance liquid chromatography, and the degradation efficiency was calculated based on the change in TC concentration before and after reaction. To clarify the role of each component in the system, different control systems were established under the same experimental conditions, including Cu^0/PDS, Cu^0/PDS/Cl^-, Cu^0/PDS/HA, Cu^0/HA/Cl^- and Cu^0/PDS/HA/Cl^- systems. These control experiments were used to compare the individual effects and the additional enhancement obtained by combining HA and Cl- on Cu^0-mediated PDS activation. Furthermore, the effects of different reaction factors on TC degradation were systematically investigated by varying HA concentration, Cl^- concentration, PDS concentration, Cu^0 dosage and initial pH while keeping the other reaction conditions unchanged. All experiments were conducted at least in triplicate, and the average values were used for subsequent data analysis.

2.3. Analytical methods

The solution pH was measured using a benchtop pH meter (PHS-25, Shanghai INESA Scientific Instrument Co., Ltd., China). The concentration of tetracycline (TC) was determined by high-performance liquid chromatography (Agilent 1260, Agilent Technologies, USA), and the detailed chromatographic conditions are provided in Text S1 (Weng et al., 2022; Xu, Feng, et al., 2025). The concentrations of Cu^+ and total dissolved copper (TDC) were determined by the neocuproine colorimetric method using a UV–vis spectrophotometer (TU-1901, Beijing Purkinje General Instrument Co., Ltd., China) at 455 nm (Oyekunle et al., 2021; Xu, Feng, et al., 2025; Xu et al., 2023). Before TDC determination, excess hydroxylamine was added to completely reduce dissolved Cu^{2+} to Cu^+, followed by measurement using the same colorimetric method (J. Wang et al., 2022; Xu, Feng, et al., 2025). The concentration of hydroxylamine (HA) was determined by a spectrophotometric method using a UV–vis spectrophotometer (TU-1901, Beijing Purkinje General Instrument Co., Ltd., China) at 705 nm (Dong et al., 2025; J. Wang et al., 2022; Xu, Feng, et al., 2025). The concentrations of NO_3^- and NO_2^- were measured using an ion chromatograph (Dionex ICS-600, Thermo Fisher Scientific Inc., USA) (Xu, Feng, et al., 2025). Total dissolved nitrogen (TDN) was determined using a total nitrogen analyzer (TN-3C/3D, Shenzhen Changhong Instrument Co., Ltd., China) (Xu, Feng, et al., 2025). Total organic carbon (TOC) was analyzed using a total organic carbon analyzer (TOC-VCPH, Shimadzu, Japan). Electron paramagnetic resonance (EPR) spectroscopy was performed using an EPR spectrometer (A200, Bruker, Germany) to detect radical signals in the system, with 5,5-dimethyl-1-pyrroline N-oxide (DMPO) used as the spin-trapping agent. The detailed experimental procedures are provided in Text S2 (Bai et al., 2026; Z.

Li et al., 2019; L. Wang et al., 2025; Weng et al., 2022). The degradation products of TC were analyzed by liquid chromatography–mass spectrometry (Agilent 1260/6550, Agilent Technologies, USA), and the detailed detection conditions are provided in Text S3 (C. Li et al., 2021; Z. Li et al., 2019; Weng et al., 2022). All experiments were conducted at least in triplicate, and the results are presented as average values.

2.4. Real water samples

Two real water samples, including tap water and surface water, were used in this study to evaluate the catalytic performance of the Cu^0/PDS/HA/Cl^- system for TC degradation.

2.5. Statistical analysis and quality control

To ensure the reliability and reproducibility of experimental data, rigorous statistical analysis and quality control were implemented for TC degradation in the Cu^0/PDS/HA/Cl^- system. The specific measures are as follows.

2.5.1. Replicates and error handling

All experimental conditions were performed at least in triplicate, and each set of results was reported as the mean ± standard deviation (SD).

The averaged data were used to generate curves, and error bars were included in figures to reflect measurement variability. Data normality was visually inspected using histograms and distribution trends to ensure suitability for subsequent statistical analyses.

2.5.2. Sample collection and treatment

At predetermined reaction times, 2.5 mL aliquots were withdrawn using a micropipette and immediately quenched with 0.5 mL of 5 mmol/L sodium thiosulfate to remove residual oxidants and stop further reaction. The quenched samples were filtered through a 0.45 μm membrane to remove suspended Cu^0 particles, ensuring accuracy for subsequent analyses.

2.5.3. Kinetic fitting and model selection

TC degradation kinetics were fitted using a pseudo-first-order model, with zero-, second-, and third-order models also compared. Fitting parameters included the apparent rate constant (k_{obs}) and the coefficient of determination (R^2). Differences in k_{obs} under various experimental conditions were compared to reflect degradation rate differences among systems.

2.5.4. Evaluation of operating factors and control systems

The effects of experimental factors (HA, Cl^-, Cu^0, PDS, pH, and reaction time) on TC degradation were systematically observed. Control systems (Cu^0/PDS, Cu^0/PDS/Cl^-, Cu^0/PDS/HA, Cu^0/HA/Cl^-, etc.) were used to compare the individual contributions and combined enhancement of each component to

degradation rates and kinetic parameters. Figures display changes in C_t/C_0, Cu^+ concentration, PDS consumption, and HA products, providing a direct visualization of variable effects on the system.

2.5.5. Quality control measures

All analytical instruments (HPLC, UV–Vis, ion chromatography) were operated according to standard procedures and calibrated with reference standards to ensure data accuracy. Sample collection and processing strictly followed operational protocols to ensure reproducibility across batches. All figures and kinetic fitting curves were generated using Origin Pro, with error bars included to reflect data variability.

3. Results and discussion

3.1. TC degradation in different reaction systems

Under matched conditions of initial pH 5.0, 0.05 g/L Cu^0, 0.1 mmol/L PDS and 5 mg/L TC (Fig. 2), the Cu^0/PDS system removed 11.1% of TC within 10 min, with an apparent rate constant (kobs) of 0.0112 min^{-1} (Z. Li et al., 2019; Xu, Feng, et al., 2025). Addition of 3 mmol/L chloride increased removal to 23.8% and kobs to 0.0263 min^{-1} (Xu, Li, et al., 2025; Xu et al., 2023). Addition of 0.3 mmol/L HA produced a larger response, with 63.8% removal and kobs of 0.1083 min^{-1} (Xu, Feng, et al., 2025). With both additives, removal reached 86.2% and kobs was 0.2119 min^{-1}. The combined system therefore outperformed each single-additive control under the tested conditions. The HA-only and chloride-only responses are consistent with the enhancement reported in related studies (Xu, Feng, et al., 2025; Xu, Li, et al., 2025; Xu et al., 2023). The additional enhancement upon combining the additives is examined here in relation to measured Cu^+ concentrations and PDS consumption (Section 3.4), rather than inferred from TC removal alone. These comparisons do not by themselves establish a quantitative synergistic interaction. Without PDS, the Cu^0/HA/Cl^- system removed only 4.9% of TC in 10 min, with kobs of 0.0044 min^{-1}, supporting the importance of PDS for the observed removal.

3.2. Effects of operating factors

3.2.1. Copper dosage

As shown in Fig. 3A, the Cu^0 dosage had an important effect on TC degradation in the Cu^0/PDS/HA/Cl^- system. As the Cu^0 dosage increased from 0.05 to 0.5 g/L, the degradation rate of TC was clearly accelerated. This improvement was mainly attributed to the enhanced generation and accumulation of Cu^+ at higher Cu^0 dosages, which further promoted PDS activation and increased the formation of reactive species, including •OH, SO_4•$^-$ and reactive chlorine species (RCS), thereby accelerating the oxidative degradation of TC (H. Li et al., 2024; Xu, Feng, et al., 2025; X. Zhou et al., 2021). Notably, the system already exhibited considerable TC removal at a Cu^0 dosage of 0.05 g/L, indicating that a relatively low Cu^0 dosage was sufficient to sustain the reaction. Therefore, considering both degradation

performance and reagent economy, 0.05 g/L Cu^0 was selected as the appropriate dosage for the Cu^0/PDS/HA/Cl^- system in subsequent experiments (T. Liu et al., 2022; Y. Zhang et al., 2023).

3.2.2. PDS concentration

As shown in Fig. 3B, the PDS concentration significantly affected TC degradation in the Cu^0/PDS/HA/Cl^- system. When the PDS concentration increased from 0 to 0.5 mmol/L, TC removal within 10 min increased markedly from 4.9% to 87.0%, indicating that increasing the PDS dosage effectively enhanced the oxidative degradation capacity of the system. This enhancement was mainly attributed to the more sufficient reaction between PDS and the generated Cu^+ at higher PDS concentrations, which accelerated the formation of reactive species, including •OH, SO_4•$^-$ and RCS, thereby strengthening the oxidative removal of TC (Feng et al., 2019; Y. Li et al., 2024; F. Liu et al., 2025; P. Zhou et al., 2018). Overall, an appropriate increase in PDS concentration was beneficial for enhancing reactive species generation in the Cu^0/PDS/HA/Cl^- system, thereby promoting TC degradation (Huang et al., 2024; L. Wang et al., 2025; Y. Yang et al., 2023).

3.2.3. HA concentration

As shown in Fig. 3C, TC degradation in the Cu^0/PDS/HA/Cl^- system first increased and then decreased with increasing HA dosage. When the HA concentration increased from 0 to 0.3 mmol/L, TC degradation within 10 min increased markedly from 20.2% to 86.1%. This result indicates that an appropriate amount of HA promoted the reduction of Cu^{2+} to Cu^+ and accelerated PDS activation, thereby generating more reactive species, including •OH, SO_4•$^-$ and RCS, and enhancing the oxidative removal of TC (Chi et al., 2019; Xu, Feng, et al., 2025; Xu et al., 2023; H. Zhang et al., 2024). However, when the HA concentration was further increased to 0.5–1.0 mmol/L, TC degradation decreased to 82.7% and 77.0%, respectively. This result suggests that although excessive HA could continuously participate in copper redox cycling, it may also act as a scavenger of reactive species and compete with TC for •OH and SO_4•$^-$, thereby reducing the amount of effective reactive species available for pollutant degradation and inhibiting TC removal (Dong et al., 2025; Y. Liu et al., 2021; Y. Liu et al., 2023; J. Wang et al., 2022). Therefore, an optimal HA dosage existed, and the best degradation performance was obtained at 0.3 mmol/L HA (H. Zhang et al., 2024; Zhong et al., 2020).

3.2.4. Chloride concentration

As shown in Fig. 3D, the Cl^- concentration had an important effect on TC degradation in the Cu^0/PDS/HA/Cl^- system. As the Cl^- concentration increased from 0 to 5 mmol/L, TC removal within 10 min increased from 63.8% to 86.2%, indicating that the introduction of Cl^- substantially enhanced the oxidative degradation capacity of the system (Oyekunle et al., 2021; Xu, Li, et al., 2025; Xu et al., 2023). This enhancement was mainly associated with the regulation of copper species transformation by Cl^-. On the one hand, Cl^- could form relatively stable $[CuCl_x]^{(1-x)}$ complexes with Cu^+, thereby suppressing

Cu^{+} disproportionation and its oxidation by dissolved oxygen. This process prolonged the persistence of Cu^{+} and improved its sustained activation of PDS (Xu, Li, et al., 2025; Xu et al., 2023). On the other hand, the presence of Cl^{-} was favorable for the formation of intermediate species such as CuCl, which further facilitated electron transfer between Cu^{0} and Cu^{2+} and accelerated the continuous generation and accumulation of Cu^{+} (X. Liu, Xin, et al., 2025; X. Liu et al., 2023).

3.2.5. Initial pH

TC removal was evaluated at initial pH values of 3, 5, 7 and 9 (Fig. 3E). The corresponding removal efficiencies after 10 min were 33.4%, 86.2%, 68.6% and 57.4%, respectively. Thus, the highest removal was obtained under weakly acidic conditions at pH 5, although the system retained activity at neutral and alkaline initial pH. This response may reflect the combined effects of pH on copper corrosion, copper speciation and competition for reactive species (Xu, Feng, et al., 2025; H. Zhang et al., 2024; Zhong et al., 2020). At higher pH, lower H^{+} availability may reduce acid-driven Cu^{0} corrosion and the supply of dissolved copper species. Meanwhile, the predominant form of HA shifts from NH_3OH^{+} to NH_2OH. Reported rate constants for NH_2OH reactions with •OH and $SO_4^{\bullet-}$ are 9.5×10^9 and 8.5×10^9 M^{-1} s^{-1}, respectively, whereas those for NH_3OH^{+} are $< 5 \times 10^8$ and 1.5×10^7 M^{-1} s^{-1} (Dong et al., 2025). HA may therefore compete more strongly with TC for reactive species at higher pH (Dong et al., 2025; H. Zhang et al., 2024). These factors provide a possible explanation for the observed pH dependence; the removal results alone do not resolve individual copper hydrolysis or surface processes.

3.3. Identification of reactive species

Reactive species were investigated using EPR spectroscopy, quenching tests and periodate-assisted UV–vis measurements (Fig. 4). The EPR spectrum showed signals assigned to $SO_4^{\bullet-}$ and •OH (Fig. 4B) (Bai et al., 2026; X. Chen et al., 2021; Z. Li et al., 2019). However, the DMPO–OH signal alone is not definitive evidence of •OH, because copper-related reactions and spin-adduct transformations may also affect the signal (Bai et al., 2026; N. Chen et al., 2022; X. Chen et al., 2021). Nitrobenzene (NB), which reacts with •OH with a reported rate constant of 3.9×10^9 M^{-1} s^{-1} and has negligible reactivity toward Cu^{3+}, was used as a probe (N. Chen et al., 2022; Fu et al., 2024). With 0.1 mmol/L NB, TC removal decreased from 86.2% to 64.5%. With 10 mmol/L tert-butanol (TBA), which can react with both •OH and Cu^{3+}, removal decreased to 63.2%. Addition of 1 mol/L methanol, a scavenger of $SO_4^{\bullet-}$ and •OH, almost completely inhibited TC degradation (Fig. 4A). These results support radical involvement, but comparisons between probes at different concentrations should not be interpreted as a precise partition of oxidant contributions. In particular, the 21.7 percentage point decrease after NB addition is an inhibition effect, rather than a directly measured 21.7% contribution from •OH; competing reactions and probe effects can influence quenching results (B. Li et al., 2024). The residual removal with NB is consistent with contributions from other oxidants. In the presence of chloride, $SO_4^{\bullet-}$ and •OH can participate in reactive chlorine species formation (X. Liu et al., 2023; Oyekunle et al., 2021; Xu, Li, et al., 2025; Xu et al., 2023). Reactive chlorine involvement is therefore mechanistically plausible, although the present tests do not quantify its individual contribution. No characteristic absorption peak at 425 nm was observed after periodate addition (Fig. 4C), providing no positive evidence for detectable Cu^{3+}–

periodate complexes under the tested conditions (N. Chen et al., 2022; Fu et al., 2024). Taken together, the tests support radical-mediated degradation and possible reactive chlorine participation, while not establishing Cu^{3+} as the dominant oxidant.

3.4. Copper cycling and combined activation mechanism

HA mainly acted as a reductive mediator in this system. It continuously reduced Cu^{2+} to Cu^{+}, thereby promoting the Cu^{+}/Cu^{2+} redox cycle and enhancing PDS activation (Chi et al., 2019; X. Liu, Yu, et al., 2025). The experimental results showed that the Cu^{+} concentration in the Cu^{0}/PDS/HA system was higher than that in the Cu^{0}/PDS system, while the PDS consumption ratio increased from 6% to 34% (Fig. 5A and 5B). These results indicate that HA addition promoted Cu+ regeneration and increased PDS consumption (Dong et al., 2025; Xu, Feng, et al., 2025). Further comparison showed that, compared with the Cu^{0}/PDS/Cl^{-} system, the Cu^{+} concentration reached the highest level in the Cu^{0}/PDS/HA/Cl^{-} system, and the PDS consumption ratio further increased from 13% to 54% (Fig. 5A and 5B). This indicates that, on the basis of Cu^{+} stabilization by Cl^{-}, HA further strengthened PDS activation through continuous Cu^{+} regeneration (X. Liu, Yu, et al., 2025; Xu, Feng, et al., 2025). Notably, HA was not rapidly depleted during the reaction. Within 10 min, the HA consumption was 0.12 mmol/L, accounting for only 40% of the initial dosage (Fig. 5C). Nitrogen balance analysis assigned 0.036 mmol/L (30%) and 0.024 mmol/L (20%) of the consumed HA nitrogen to nitrate and nitrite, respectively. The remaining 0.060 mmol/L (50%) was attributed to gaseous nitrogen products such as N_2/N_2O (Dong et al., 2025; J. Wang et al., 2022; Xu, Feng, et al., 2025); this balance does not distinguish the individual gaseous products. The partial consumption of HA shows that reductant remained available after 10 min. It supports continued Cu^{2+} reduction during the reaction, but does not demonstrate HA regeneration or a non-sacrificial catalytic role (Dong et al., 2025; Xu, Feng, et al., 2025). Cl^{-} mainly enhanced the system by stabilizing Cu^{+} and promoting its effective utilization (X. Liu et al., 2023; Xu, Li, et al., 2025; Xu et al., 2023). Previous studies had shown that free Cu^{+} readily underwent disproportionation in aqueous solution and can also be oxidized by dissolved oxygen, which limited its role in PDS activation (Z. Li et al., 2019; X. Liu et al., 2023). However, as an important ligand for Cu^{+}, Cl^{-} can form $[CuCl_x]^{(1-x)}$ complexes with Cu^{+}. Compared with free Cu^{+}, these complexes have higher stability and can effectively suppress Cu^{+} disproportionation and its side reaction with dissolved oxygen, with the related reaction rate constants being 3.1×10^{4}, 19, 0.12 and 0.44 $M^{-1}\ s^{-1}$, respectively (X. Liu et al., 2023; Oyekunle et al., 2021; Xu et al., 2023). Therefore, Cl^{-} addition not only reduced the ineffective loss of Cu^{+}, but also increased the measured Cu+ concentration in the system, thereby enhancing its ability to activate PDS (Xu, Li, et al., 2025). To further verify the comproportionation reaction between Cu^{2+} and Cu^{0} in the presence of Cl^{-}, the different concentrations of Cu^{2+} were added to a system containing 0.2 g/L Cu^{0} and 5 mmol/L Cl^{-}, and the changes in Cu^{+} concentration and TC removal were monitored. Figure S2 shows higher Cu^{+} accumulation with 0.2 mmol/L Cu^{2+} than with 0.1 mmol/L Cu^{2+}, while the TC removal response does not increase in parallel. The Cu^{+} trend is consistent with Cu^{0}/Cu^{2+} comproportionation in the chloride-containing system, but should not be interpreted as a monotonic improvement in TC removal (X. Liu et

al., 2023; Xu, Li, et al., 2025; Xu et al., 2023). These measurements show concurrent changes in Cu^{+} availability, PDS consumption and TC removal across the matched controls. PDS consumption was 6% without either additive, 34% with HA, 13% with chloride and 54% with both. Greater PDS consumption alone does not establish improved oxidant utilization efficiency, because productive oxidation and competing reactions both consume PDS. The Cu^{+} measurements also do not directly resolve free Cu^{+} from individual chloride complexes. On this basis, the proposed reinforcement mechanism of the Cu^{0}/PDS/HA/Cl^{-} system can be summarized as follows (Fig. 6). First, Cu^{0} released Cu^{+} through reactions with PDS, O_2 and H^{+} (Wen et al., 2014; Xu, Feng, et al., 2025; P. Zhou et al., 2018). Subsequently, Cu^{+} and its Cl^{-}-complexed species, $[CuCl_x]^{(1-x)}$, jointly participated in PDS activation to generate $SO_4^{\bullet -}$ and •OH, and further induced the formation of RCS, thereby accelerating TC degradation. Meanwhile, HA continuously reduced Cu^{2+} to Cu^{+}; Cl^{-} increased the measured Cu+ concentration through complexation stabilization and promotion of the comproportionation reaction (X. Liu, Yu, et al., 2025; Xu, Feng, et al., 2025). The combined-additive response is consistent with complementary Cu^{+} generation and stabilization, accompanied by increased PDS consumption and TC removal (X. Liu, Yu, et al., 2025; Xu, Feng, et al., 2025; Xu et al., 2023).

Table 1

Reaction pathways of PDS activation and reactive species generation in the Cu^0/PDS/HA/Cl^- system.

No.	Reaction	Rate or equilibrium parameter	References
1	$2Cu^0 + 2H^+ \rightarrow 2Cu^+ + H_2$	NA	(Z. Li et al., 2019)
2	$Cu^0 + S_2O_8^{2-} \rightarrow Cu^+ + SO_4^{\bullet -} + SO_4^{2-}$	NA	(Z. Li et al., 2019)
3	$2Cu^{2+} + NH_2OH \rightarrow 2Cu^+ + HNO + 2H^+$	ND	(Xu et al., 2023)
4	$Cu^0 + Cu^{2+} + 2Cl^- \rightarrow 2CuCl$	ND/NA	(Xu et al., 2023)
5	$Cu^+ + Cl^- \rightleftharpoons CuCl$	$\log\beta_1 = 3.10$	(Xu et al., 2023)
6	$Cu^+ + 2Cl^- \rightleftharpoons CuCl_2^-$	$\log\beta_2 = 5.68$	(Xu et al., 2023)
7	$Cu^+ + 3Cl^- \rightleftharpoons CuCl_3^{2-}$	$\log\beta_3 = 5.02$	(Xu et al., 2023)
8	$Cu^+ + S_2O_8^{2-} \rightarrow Cu^{2+} + SO_4^{\bullet -} + SO_4^{2-}$	$k = 1.0 \times 10^7\ M^{-1}\ s^{-1}$	(Lu et al., 2026)
9	$CuCl_x^{(1-x)} + S_2O_8^{2-} \rightarrow Cu^{2+} + xCl^- + SO_4^{\bullet -} + SO_4^{2-}$	ND	(Z. Li et al., 2019)
10	$SO_4^{\bullet -} + H_2O \rightarrow {\bullet}OH + SO_4^{2-} + H^+$	$k = 2.0 \times 10^2\ s^{-1}$	(Xu et al., 2023)
11	$SO_4^{\bullet -} + OH^- \rightarrow {\bullet}OH + SO_4^{2-}$	$k = 6.5 \times 10^7\ M^{-1}\ s^{-1}$	(Xu et al., 2023)
12	$SO_4^{\bullet -} + Cl^- \rightarrow SO_4^{2-} + Cl{\bullet}$	$k = 2.7 \times 10^8\ M^{-1}\ s^{-1}$	(Xu et al., 2023)
13	$Cl^- + {\bullet}OH \rightarrow ClOH^{\bullet -}$	$k = 4.3 \times 10^9\ M^{-1}\ s^{-1}$	(X. Liu et al., 2023)
14	$ClOH^{\bullet -} + H^+ \rightarrow Cl{\bullet} + H_2O$	$k = 2.1 \times 10^{10}\ M^{-1}\ s^{-1}$	(X. Liu et al., 2023)
15	$Cl{\bullet} + Cl^- \rightarrow Cl_2^{\bullet -}$	$k = 6.5 \times 10^9\ M^{-1}\ s^{-1}$	(X. Liu et al., 2023)

Note: NA indicates that the reaction is not applicable to a homogeneous second-order rate constant because it is heterogeneous or surface-mediated. ND indicates that the parameter has not been directly determined or reported. β represents the cumulative formation constant of Cu(I)-chloride complexes.

Figure 6 Reaction mechanism of HA/Cl^--enhanced Cu^0/PDS activation for tetracycline degradation. Reaction conditions: $[TC]_0$ = 5 mg/L, $[Cu^0]_0$ = 0.05 g/L, $[HA]_0$ = 0.3 mmol/L, $[PDS]_0$ = 0.1 mmol/L, $[Cl^-]_0$ = 3 mmol/L, pH = 5.0 ± 0.1, T = 25 ± 1°C

3.5. Water matrix effects and application limitations

Various dissolved inorganic anions are commonly present in real aquatic environments, and these coexisting components may interfere with pollutant removal in advanced oxidation systems. Therefore, it is important to investigate the effects of water matrix components on TC degradation in the Cu^0/PDS/HA/Cl^- system (He et al., 2023; C. Li et al., 2021; P. Zhou et al., 2018). As shown in Fig. 7A, when the concentrations of CO_3^{2-}, NO_3^-, PO_4^{3-} and SO_4^{2-} were all 2 mmol/L, these anions showed only limited inhibition of TC removal, indicating that the Cu^0/PDS/HA/Cl^- system had relatively strong tolerance to common inorganic ions. In contrast, after the addition of 2 mmol/L fulvic acid, TC degradation efficiency decreased markedly from 86.2% to 57.3%. This result indicated that fulvic acid had an obvious inhibitory effect on the reaction system, mainly because it could act as a radical scavenger and compete with TC for •OH, SO_4•$^-$ and RCS, thereby weakening the oxidative degradation of TC by reactive species (Y. Li et al., 2024; Xu, Feng, et al., 2025; P. Zhou et al., 2018). Furthermore, the application performance of Cu^0/PDS/HA/Cl^- system was evaluated in real water samples. As shown in Fig. 7B, the TC removal efficiencies in tap water and surface water were 77.1% and 67.7% within 10 min, respectively, both of which were lower than that obtained in the ideal aqueous system. This inhibition was likely due to the competitive consumption of reactive species, including SO_4•$^-$, •OH and RCS, by natural organic matter and other matrix components in real water samples (Chi et al., 2019; C. Li et al., 2021; P. Zhou et al., 2018). Nevertheless, the system still achieved more than 67% TC removal within 10 min in real water samples, indicating its oxidative degradation potential and application prospects in complex aquatic environments (He et al., 2023; C. Li et al., 2021). TOC removal was only 5.7% after 10 min, compared with 86.2% TC removal, indicating limited mineralization (X. Chen et al., 2021; Y. Li et al., 2024). Thus, disappearance of the parent antibiotic should not be equated with complete organic carbon removal or demonstrated detoxification. The proposed transformation pathway and LC-MS assignments are provided in Fig. S1 and Table S3. After three reuse cycles, Cu^0 retained TC removal above 82% (Fig. S3), indicating activity retention over the tested cycles (Z. Li et al., 2019; T. Liu et al., 2022; Xu et al., 2023). Notably, after TC treatment by the Cu^0/PDS/HA/Cl^- system, the total dissolved copper (TDC) concentration was 7.16 mg/L. Because copper release requires control in water treatment, alkaline precipitation followed by filtration was applied to the reacted solution (X. Liu et al., 2023; Xu et al., 2023). After adjustment to pH 9.0 and filtration through a 0.45 μm membrane, TDC decreased to 0.673 mg/L (Fig. S4). This demonstrates dissolved copper removal by post-treatment, but does not by itself establish compliance with wastewater discharge requirements. A surface water environmental quality benchmark is distinct from an effluent discharge limit, and assessment of practical use must also consider residual reagents, transformation products and copper-containing solids (X. Liu et al., 2023; Oyekunle et al., 2021; Xu et al., 2023). Compared with conventional iron-based zero-valent metal systems, Cu^0-based oxidation processes exhibit distinct characteristics in regulating metal redox processes during persulfate activation. Although Fe^0 systems have attracted extensive attention owing to their low cost and abundance, their practical applications may be limited by surface passivation and metal sludge formation under certain conditions (Kaur et al., 2023; Liang et al., 2023; Shi et al., 2025; X. Zhou et al.,

2024). In contrast, Cu^0-based systems provide effective pathways for regulating metal redox cycling during persulfate activation (Ding et al., 2022; Xu et al., 2023). Nevertheless, appropriate consideration of copper management remains necessary for practical applications. The present tap water and surface water tests support further evaluation of the process, rather than demonstrating full-scale wastewater treatment readiness. Further work should assess mineralization, transformation-product toxicity, potential chlorinated by-products and management of copper-containing solids.

4. Conclusions

HA and chloride enhanced TC removal by the Cu^0/PDS system through complementary regulation of copper cycling. Under the selected conditions ($[TC]_0$ = 5 mg/L, $[Cu^0]_0$ = 0.05 g/L, $[HA]_0$ = 0.3 mmol/L, $[PDS]_0$ = 0.1 mmol/L, $[Cl^-]_0$ = 3 mmol/L and initial pH 5.0), TC removal reached 86.2% within 10 min, compared with 11.1% in Cu^0/PDS, 63.8% with HA alone and 23.8% with chloride alone. The apparent rate constant was 0.2119 min^{-1}. The highest performance occurred at pH 5.0, while removal at initial pH 7.0 was 68.6%.

The matched-control comparison connects the combined-additive enhancement to measured Cu^+ concentrations and PDS consumption. PDS consumption was 6% in Cu^0/PDS, 34% with HA, 13% with chloride and 54% with both additives. These concurrent responses are consistent with complementary HA-assisted Cu^{2+} reduction and chloride-mediated Cu^+ stabilization, but do not directly resolve individual Cu(I) complexes or quantify an interaction between the additives. HA consumption was 40% of the initial dosage over 10 min, showing partial reductant consumption rather than proving HA regeneration. The reactive species tests support radical involvement and possible reactive chlorine participation, while not establishing Cu^{3+} as the dominant oxidant. The quenching results do not provide a quantitative partition of individual oxidant contributions.

TC removal reached 77.1% in tap water and 67.7% in surface water, and remained above 82% over three copper reuse cycles. However, 5.7% TOC removal after 10 min indicates limited mineralization. Alkaline precipitation and filtration reduced TDC from 7.16 to 0.673 mg/L, demonstrating the value of a separate copper removal step. The combined process is a candidate for further investigation in antibiotic-contaminated water treatment. Its practical assessment requires additional evidence on transformation-product toxicity, potential chlorinated by-products, residual reagents and management of copper-containing solids.

Declarations

Competing interests

The authors declare that they have no known competing financial interests or personal relationships that could have appeared to influence the work reported in this paper.

Supplementary material

Online Resource 1 contains analytical procedures (Texts S1–S3), instrument and water matrix information (Tables S1–S2), LC-MS assignments (Table S3), and figures on the proposed degradation pathway, copper speciation, reuse and post-treatment (Figs. S1–S4).

Funding

This work was supported by the Hunan Provincial Natural Science Foundation of China [grant numbers 2025JJ50181, 2023JJ40288 and 2024JJ8319].

Author Contribution

R.D., C.W., and S.Z. provided funding support. R.D. and X.L. contributed to the methodology and reviewed and edited the manuscript. Q.Y. was responsible for manuscript writing and software. B.H., X.W., B.R., S.L., and W.H. contributed to the methodology.

References

1. Bai, S., Wang, P., Xu, C., Wang, L., Hu, X., Hu, P., Fu, Y., & Wang, Z. (2026). Dimethyl sulfoxide as a qualitative EPR indicator of sulfate radical in advanced oxidation processes. *Water Research*, *289*, Article 125011. https://doi.org/10.1016/j.watres.2025.125011
2. Chen, N., Lee, D., Kim, M. S., Shang, H., Cao, S., Park, E. J., Li, M., Zhang, L., & Lee, C. (2022). Activation of molecular oxygen by tenorite and ascorbic acid: Generation of high-valent copper species for organic compound oxidation. *Journal of Hazardous Materials*, *440*, Article 129839. https://doi.org/10.1016/j.jhazmat.2022.129839
3. Chen, X., Zhou, J., Chen, Y., Zhou, Y., Ding, L., Liang, H., & Li, X. (2021). Degradation of tetracycline hydrochloride by coupling of photocatalysis and peroxymonosulfate oxidation processes using CuO-BiVO4 heterogeneous catalyst. *Process Safety and Environmental Protection*, *145*, 364–377. https://doi.org/10.1016/j.psep.2020.08.016
4. Chen, Y., Ge, X., Wang, R., Zhao, Q., Ye, Z., & Li, Z. (2025). WS2 promotes peroxymonosulfate activation by zero-valent Cu for micropollutant degradation: Excellent applicability and interfacial electron transfer mechanisms. *Separation and Purification Technology*, *368*, Article 132987. https://doi.org/10.1016/j.seppur.2025.132987
5. Chi, H., He, X., Zhang, J., & Ma, J. (2019). Efficient degradation of refractory organic contaminants by zero-valent copper/hydroxylamine/peroxymonosulfate process. *Chemosphere*, *237*, Article 124431. https://doi.org/10.1016/j.chemosphere.2019.124431
6. Ding, Y., Fu, L., Peng, X., Lei, M., Wang, C., & Jiang, J. (2022). Copper catalysts for radical and nonradical persulfate based advanced oxidation processes: Certainties and uncertainties. *Chemical*

Engineering Journal, *427*, Article 131776. https://doi.org/10.1016/j.cej.2021.131776

7. Dong, Z. J., Jiang, C. C., Zhou, Y., Ning, Y. Y., Sun, X. H., & Lv, G. (2025). Hydroxylamine-driven advanced oxidation process: Impact of key environmental factors on active species, reaction pathways, and kinetics. *Separation and Purification Technology*, *354*, Article 129063. https://doi.org/10.1016/j.seppur.2024.129063
8. Du, X., Zhang, Y., Hussain, I., Huang, S., & Huang, W. (2017). Insight into reactive oxygen species in persulfate activation with copper oxide: Activated persulfate and trace radicals. *Chemical Engineering Journal*, *313*, 1023–1032. https://doi.org/10.1016/j.cej.2016.10.138
9. Feng, Y., Qing, W., Kong, L., Li, H., Wu, D., Fan, Y., Lee, P. H., & Shih, K. (2019). Factors and mechanisms that influence the reactivity of trivalent copper: A novel oxidant for selective degradation of antibiotics. *Water Research*, *149*, 1–8. https://doi.org/10.1016/j.watres.2018.10.090
10. Fu, J., Li, H., Jiang, G., Feng, D., Yi, J., Liu, Y., Gong, R., Guo, J., Liu, P., & Cui, K. (2024). Enhanced removal of tetracycline hydrochloride by activation of persulfate with sludge-red mud magnetic biochar: Synergistic effect between adsorption and radical-nonradical pathways. *Inorganic Chemistry Communications*, *170*, Article 113451. https://doi.org/10.1016/j.inoche.2024.113451
11. He, H., Xiao, H., Liu, C., Li, Y., Li, D., Li, M., & Liu, Y. (2023). Efficient degradation of tetracycline with N-rGO/CuO catalysts under high salinity condition via persulfate activation dominated by non-radical pathways. *Separation and Purification Technology*, *327*, Article 124936. https://doi.org/10.1016/j.seppur.2023.124936
12. Huang, X., Wang, X., Xu, H., Zhang, Y., Zheng, G., Yang, Z., Ye, Q., Wang, Y., & Zhang, J. (2024). Oxidation of tetracycline hydrochloride by peroxomonosulfate and peroxodisulfate on a ZnNi@NC carbonaceous catalyst: Role of non-radical species and mediated or direct electron transfer mechanisms. *Process Safety and Environmental Protection*, *181*, 75–86. https://doi.org/10.1016/j.psep.2023.10.054
13. Kaur, P., Kumar, A., Babu, J. N., & Kumar, S. (2023). Tetracycline removal via three-way synergy between pistachio shell powder, zerovalent copper or iron, and peroxymonosulfate activation. *Journal of Hazardous Materials Advances*, *12*, Article 100385. https://doi.org/10.1016/j.hazadv.2023.100385
14. Li, B., Chen, B., & Wei, Z. (2024). Challenging established norms: The unanticipated role of alcohols in UV/PDS radical quenching. *Journal of Hazardous Materials*, *478*, Article 135502. https://doi.org/10.1016/j.jhazmat.2024.135502
15. Li, C., Goetz, V., & Chiron, S. (2021). Peroxydisulfate activation process on copper oxide: Cu(III) as the predominant selective intermediate oxidant for phenol and waterborne antibiotics removal. *Journal of Environmental Chemical Engineering*, *9*, Article 105145. https://doi.org/10.1016/j.jece.2021.105145
16. Li, H., Sun, H., Li, Q., Zong, X., Wu, L., Han, Z., Li, X., Wu, J., Ye, Y., & Pan, F. (2024). Copper-doped orange peel biochar activated peroxydisulfate for efficient degrading tetracycline: The critical role of

C-OH and Cu. *Environmental Research*, *263*, Article 120265. https://doi.org/10.1016/j.envres.2024.120265

17. Li, Y., Zhang, C., Zhao, G., Su, P., Wang, J., Li, Y., Zhou, W., Mu, Y., Zhang, J., & Liu, W. (2024). A critical review on antibiotics removal by persulfate-based oxidation: Activation methods, catalysts, oxidative species, and degradation routes. *Process Safety and Environmental Protection*, *187*, 622–643. https://doi.org/10.1016/j.psep.2024.05.001
18. Li, Z., Guo, C., Lyu, J., Hu, Z., & Ge, M. (2019). Tetracycline degradation by persulfate activated with magnetic Cu/CuFe2O4 composite: Efficiency, stability, mechanism and degradation pathway. *Journal of Hazardous Materials*, *373*, 85–96. https://doi.org/10.1016/j.jhazmat.2019.03.075
19. Liang, F., Liu, Z., Jiang, X., Li, J., Xiao, K., Xu, W., Chen, X., Liang, J., Lin, Z., Li, M., Wu, X., & Wang, H. (2023). NaOH-modified biochar supported Fe/Mn bimetallic composites as efficient peroxymonosulfate activator for enhance tetracycline removal. *Chemical Engineering Journal*, *454*, Article 139949. https://doi.org/10.1016/j.cej.2022.139949
20. Liu, F., He, G., Yu, F., & Wu, X. (2025). Activation of peroxymonosulfate by cobalt-iron nanoparticles anchored on nitrogen-doped biochar for efficient removal of tetracycline from water: Free radical and non-free radical pathways. *Process Safety and Environmental Protection*, *203*, Article 107856. https://doi.org/10.1016/j.psep.2025.107856
21. Liu, T., Yin, K., Li, N., Liu, H., Chen, J., Zhou, X., & Zhang, Y. (2022). Efficient activation of peroxymonosulfate by copper supported on polyurethane foam for contaminant degradation: Synergistic effect and mechanism. *Chemical Engineering Journal*, *427*, Article 131741. https://doi.org/10.1016/j.cej.2021.131741
22. Liu, X., Xin, Q., Yu, Q., Peng, R., Zeng, T., & Xu, P. (2025). Enhanced degradation of acetaminophen by zero-valent copper coupled with hydroxylamine in the presence of chloride ions. *Journal of Water Process Engineering*, *78*, Article 108836. https://doi.org/10.1016/j.jwpe.2025.108836
23. Liu, X., Xu, P., Xie, S., Wang, L., Yang, Z., Zhu, P., Ma, J., He, Q., & Crittenden, J. C. (2023). Multiple reinforcement of chloride ion on oxidizing acetaminophen with zero-valent copper particles: In-site formation and catalysis of hydrogen peroxide. *Chemical Engineering Journal*, *451*, Article 138689. https://doi.org/10.1016/j.cej.2022.138689
24. Liu, X., Yu, Q., Xu, P., Ma, J., He, Q., & Zheng, M. (2025). Combination of hydroxylamine and chloride ion driven the zero-valent copper-triggered hydrogen peroxide process for efficient decomposition of tetracycline. *Process Safety and Environmental Protection*, *201*, Article 107526. https://doi.org/10.1016/j.psep.2025.107526
25. Liu, Y., Miao, W., Feng, Y., Fang, X., Li, Q., Du, N., Wang, D., & Mao, S. (2021). Enhanced peroxydisulfate oxidation via Cu(III) species with a Cu-MOF-derived Cu nanoparticle and 3D graphene network. *Journal of Hazardous Materials*, *403*, Article 123691. https://doi.org/10.1016/j.jhazmat.2020.123691
26. Liu, Y., Wang, X., Sun, Q., Chen, L., Yuan, M., Sun, Z., Zhang, Y., Xia, S., & Zhao, J. (2023). Enhanced activation of peroxymonosulfate by a floating Cu0-MoS2/C3N4 photocatalyst under visible-light

assistance for tetracyclines degradation and Escherichia coli inactivation. *Chemical Engineering Journal*, *457*, Article 141220. https://doi.org/10.1016/j.cej.2022.141220

27. Lu, B., Wu, J., Tang, C., Zou, J., Sun, B., Wang, M., Cheng, Q., Tan, H., Li, Q., & Ma, J. (2026). Facilitating redox cycles of copper species by peroxydisulfate in the copper-catalyzed Fenton-like system for enhanced oxidation of organic contaminants. *Water Research*, *289*, Article 124839. https://doi.org/10.1016/j.watres.2025.124839
28. Niu, J., Jia, H., Yu, M., Zhu, J., Ma, J., He, Z., Zhong, W., Hou, Y., & Guo, Y. (2024). Nitrogen-rich penicillin residue biochar for activation of peroxymonosulfate for an efficient degradation of tetracycline and its dual-pathway mechanism. *Process Safety and Environmental Protection*, *182*, 416–425. https://doi.org/10.1016/j.psep.2023.11.066
29. Oyekunle, D. T., Cai, J., Gendy, E. A., & Chen, Z. (2021). Impact of chloride ions on activated persulfates based advanced oxidation process (AOPs): A mini review. *Chemosphere*, *280*, Article 130949. https://doi.org/10.1016/j.chemosphere.2021.130949
30. Shi, Q., Feng, Y., Wang, W., Xu, Z., Li, Z., & Zhu, W. (2025). Porous biochar encapsulating highly dispersed Co3O4 as peroxymonosulfate activator for the enhanced tetracycline removal. *Process Safety and Environmental Protection*, *196*, Article 106947. https://doi.org/10.1016/j.psep.2025.106947
31. Wang, J., Zhang, Q., Peng, J., Wei, Z., Li, Y., & Wu, X. (2022). Persulfate activation by copper tailings with hydroxylamine: efficiency, mechanism and DFT calculations. *Separation and Purification Technology*, *297*, Article 121472. https://doi.org/10.1016/j.seppur.2022.121472
32. Wang, L., Tang, Y., Wang, P., Fu, Y., Xu, C., & Wang, Z. (2025). Radical generation in thermally activated peroxydisulfate process with temperature threshold as low as 45°C. *Chemical Engineering Journal*, *526*, Article 171071. https://doi.org/10.1016/j.cej.2025.171071
33. Wen, G., Wang, S. J., Ma, J., Huang, T. L., Liu, Z. Q., Zhao, L., & Xu, J. L. (2014). Oxidative degradation of organic pollutants in aqueous solution using zero valent copper under aerobic atmosphere condition. *Journal of Hazardous Materials*, *275*, 193–199. https://doi.org/10.1016/j.jhazmat.2014.05.002
34. Weng, M., Cai, M., Xie, Z., Dong, C., Zhang, Y., Song, Z., Shi, Y., Jin, M., Wang, Q., & Wei, Z. (2022). Hydrodynamic cavitation-enhanced heterogeneous activation of persulfate for tetracycline degradation: Synergistic effects, degradation mechanism and pathways. *Chemical Engineering Journal*, *431*, Article 134238. https://doi.org/10.1016/j.cej.2021.134238
35. Xu, P., Feng, J., Li, N., Yao, J., Li, G., & Hou, B. (2025). Hydroxylamine enhanced zero-valent copper/persulfate oxidation systems: Rapid corrosion of Cu(0) and reduction of Cu(□). *Journal of Environmental Chemical Engineering*, *13*, Article 115615. https://doi.org/10.1016/j.jece.2025.115615
36. Xu, P., Li, N., Zhu, P., & Wu, R. (2025). The effect of chloride ion on the reinforcement of zero-valent copper activated peroxysulphate. *Journal of Water Process Engineering*, *71*, Article 107409. https://doi.org/10.1016/j.jwpe.2025.107409

37. Xu, P., Zhu, P., Yang, Z., Liu, X., Wu, R., & Hou, B. (2023). Chloride ion with ferric ion in boosting zero-valent copper activated peroxydisulfate for efficiently removing tetracycline. *Chemical Engineering Journal*, *471*, Article 144773. https://doi.org/10.1016/j.cej.2023.144773
38. Yang, X., Zhang, X., Wang, J., Zhang, J., & Bai, H. (2024). Efficient and easy-to-recover immobilized heterogeneous catalyst CuSF/ZIF-67 activates peroxymonosulfate to remove refractory antibiotics. *Process Safety and Environmental Protection*, *192*, 769–781. https://doi.org/10.1016/j.psep.2024.10.098
39. Yang, Y., Lin, J., Liu, Z., & Liu, M. (2023). Degradation of tetracycline by peroxydisulfate activation on sludge-derived biochar modified with tannin extract. *Process Safety and Environmental Protection*, *173*, 472–484. https://doi.org/10.1016/j.psep.2023.03.003
40. Zhang, H., Wang, X., Lin, Y., Lv, Y., Chen, L., & Wang, L. (2024). Highly-efficient peroxymonosulfate activation by porous nano-MgO for tetracycline degradation: Surface hydroxyl groups and oxygen vacancies synergetic mediated nonradical process. *Process Safety and Environmental Protection*, *190*, 560–573. https://doi.org/10.1016/j.psep.2024.07.082
41. Zhang, X., Cai, T., Zhang, S., Hou, J., Cheng, L., Chen, W., & Zhang, Q. (2024). Contamination distribution and non-biological removal pathways of typical tetracycline antibiotics in the environment: A review. *Journal of Hazardous Materials*, *463*, Article 132862. https://doi.org/10.1016/j.jhazmat.2023.132862
42. Zhang, Y., Wu, M., Yi, Y., Sun, P., & Dong, X. (2023). A non-radical activation of peroxydisulfate by CuO to selectively oxidize aminobenzenes to nitrobenzenes. *Journal of Environmental Chemical Engineering*, *11*, Article 110729. https://doi.org/10.1016/j.jece.2023.110729
43. Zhong, Q., Lin, Q., Huang, R., Fu, H., Zhang, X., Luo, H., & Xiao, R. (2020). Oxidative degradation of tetracycline using persulfate activated by N and Cu codoped biochar. *Chemical Engineering Journal*, *380*, Article 122608. https://doi.org/10.1016/j.cej.2019.122608
44. Zhou, P., Zhang, J., Zhang, Y., Zhang, G., Li, W., Wei, C., Liang, J., Liu, Y., & Shu, S. (2018). Degradation of 2,4-dichlorophenol by activating persulfate and peroxomonosulfate using micron or nanoscale zero-valent copper. *Journal of Hazardous Materials*, *344*, 1209–1219. https://doi.org/10.1016/j.jhazmat.2017.11.023
45. Zhou, X., Guo, Z., Tang, X., Wang, W., Wu, M., Song, B., Xiang, Y., Li, Y., Xiong, W., Huang, D., & Zhou, C. (2024). Sulfate radical-based advanced oxidation processes for simultaneous removal of antibiotic-resistant bacteria and antibiotic resistance genes and the affecting factors. *Chemical Engineering Journal*, *498*, Article 155149. https://doi.org/10.1016/j.cej.2024.155149
46. Zhou, X., Luo, H., Sheng, B., Chen, X., Wang, Y., Chen, Q., & Zhou, J. (2021). Cu2+/Cu+ cycle promoted PMS decomposition with the assistance of Mo for the degradation of organic pollutant. *Journal of Hazardous Materials*, *411*, Article 125050. https://doi.org/10.1016/j.jhazmat.2021.125050

Figures

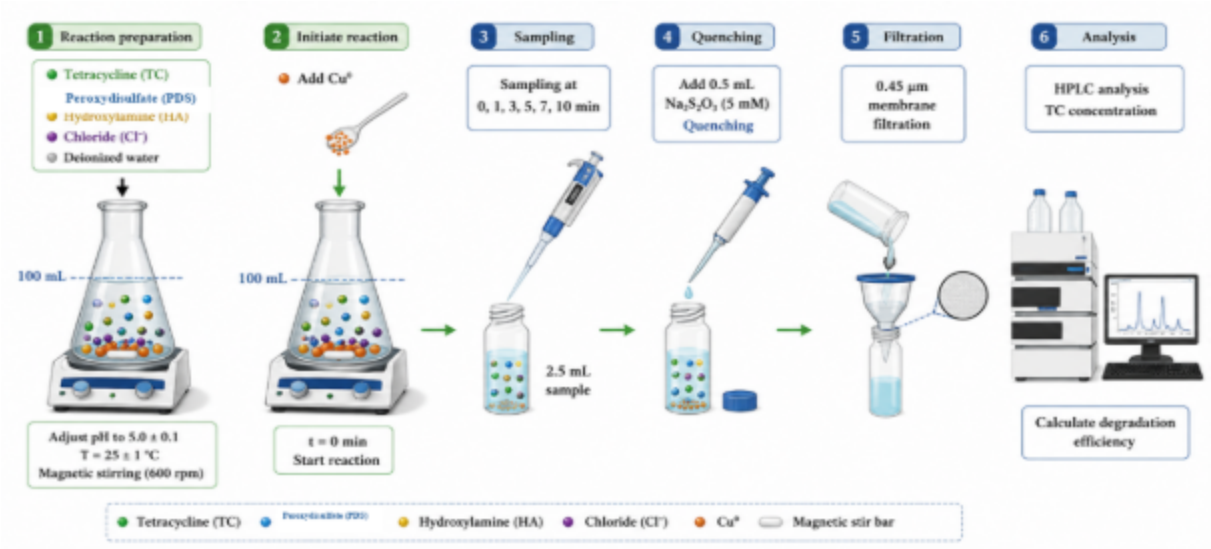


Figure 1

Experimental procedure for tetracycline degradation and analysis

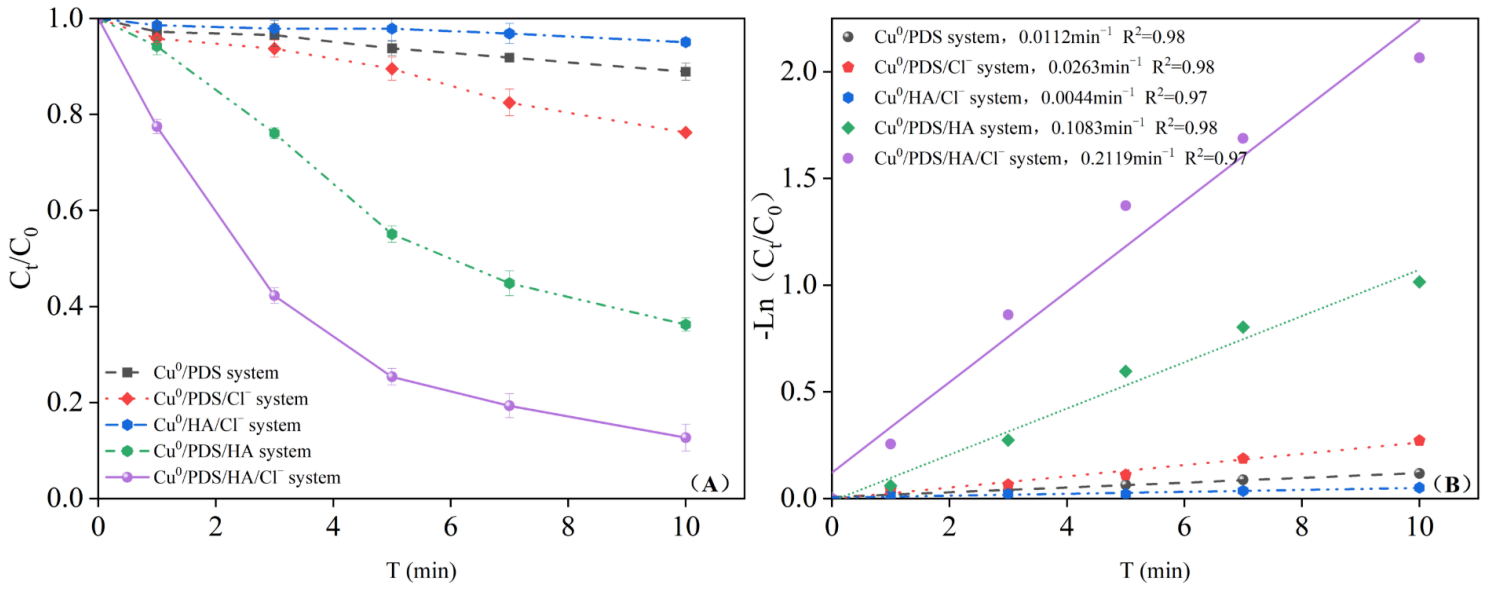


Figure 2

Degradation of TC in different reaction systems. Reaction conditions: $[TC]_0$ = 5 mg/L, $[Cu^0]_0$ = 0.05 g/L, $[HA]_0$ = 0.3 mmol/L, $[PDS]_0$ = 0.1 mmol/L, $[Cl^-]_0$ = 3 mmol/L, pH = 5.0 ± 0.1, T = 25 ± 1 °C

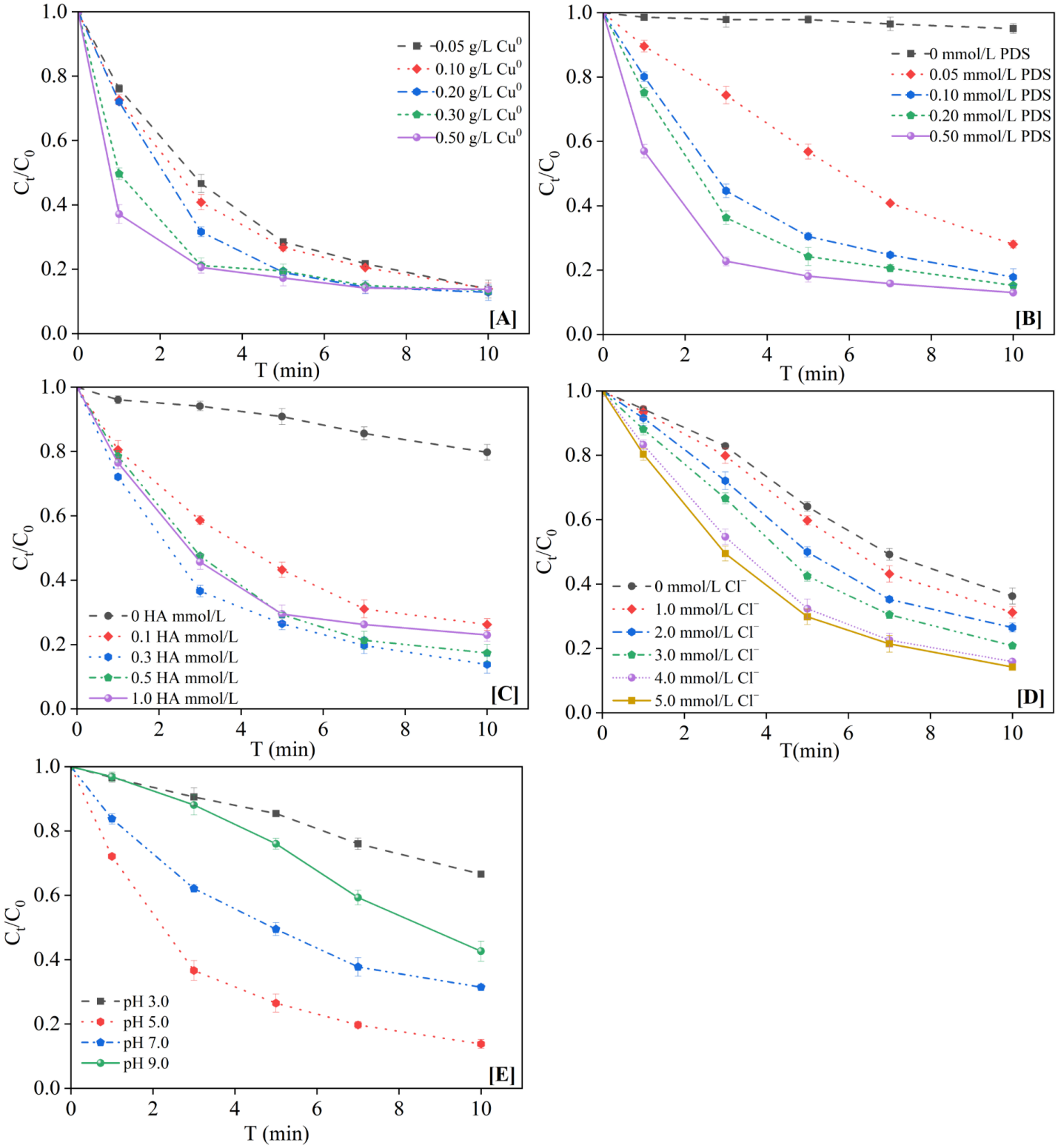


Figure 3

Effects of Cu^0 dosage (A), PDS (B), HA (C), Cl^- (D), and initial pH (E) on TC degradation in the Cu^0/PDS/HA/Cl^- system. Reaction conditions: $[TC]_0$ = 5 mg/L; $[Cu^0]_0$ = 0.05, 0.1, 0.2, 0.3 and 0.5 g/L; $[HA]_0$ = 0, 0.1, 0.3, 0.5 and 1 mmol/L; $[PDS]_0$ = 0, 0.05, 0.1, 0.2 and 0.5 mmol/L; $[Cl^-]_0$ = 0, 1, 2, 3, 4 and 5 mmol/L; pH_0 = 3.0, 5.0, 7.0, 9.0; T = 25 ± 1 °C

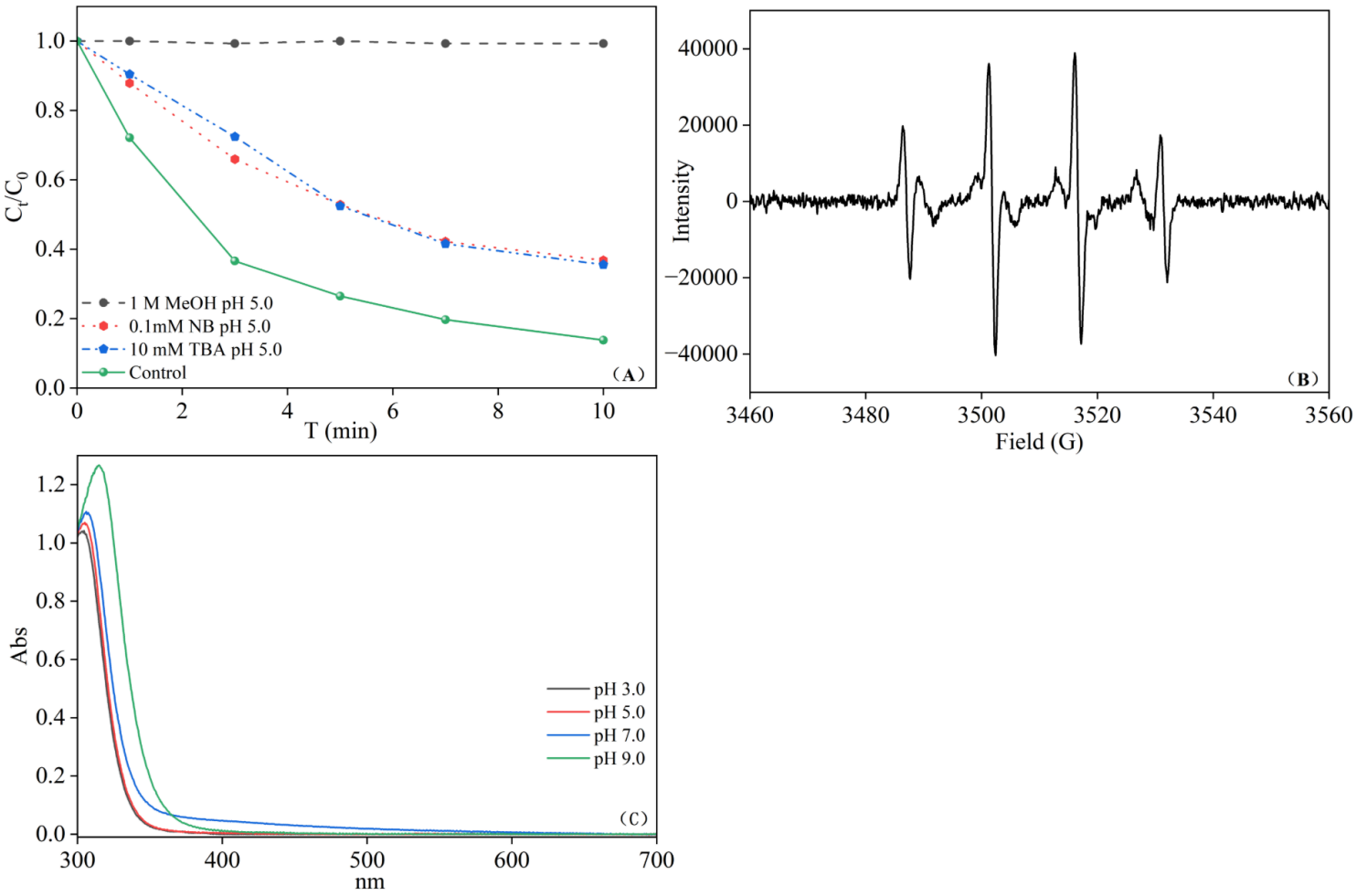


Figure 4

Effects of methanol, nitrobenzene and tert-butanol on TC degradation (A), EPR spectra of the Cu^0/PDS/HA/Cl^- system with DMPO as the spin-trapping agent (B), and UV–vis spectra of the system after periodate addition at different pH (C). Reaction conditions: $[TC]_0$ = 5 mg/L, $[Cu^0]_0$ = 0.05 g/L, $[HA]_0$ = 0.3 mmol/L, $[PDS]_0$ = 0.1 mmol/L, $[Cl^-]_0$ = 3 mmol/L, pH = 5.0 ± 0.1, T = 25 ± 1 °C

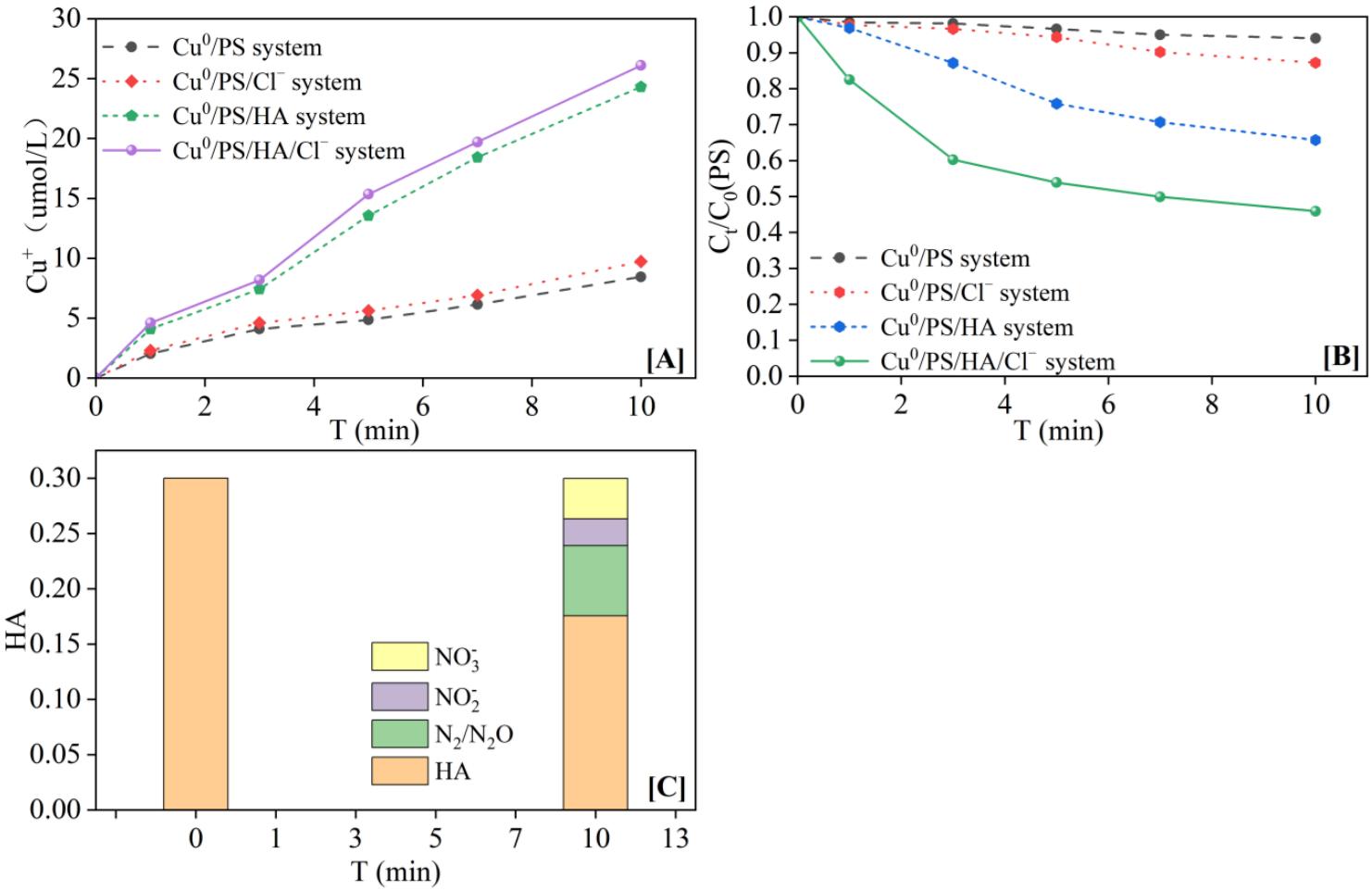


Figure 5

Changes in Cu^+ concentration (A) and PDS consumption (B), and transformation products of HA (C). Reaction conditions: $[TC]_0$ = 5 mg/L, $[Cu^0]_0$ = 0.05 g/L, $[HA]_0$ = 0.3 mmol/L, $[PDS]_0$ = 0.1 mmol/L, $[Cl^-]_0$ = 3 mmol/L, pH = 5.0 ± 0.1, T = 25 ± 1 °C. PS in the panel labels denotes peroxydisulfate (PDS)

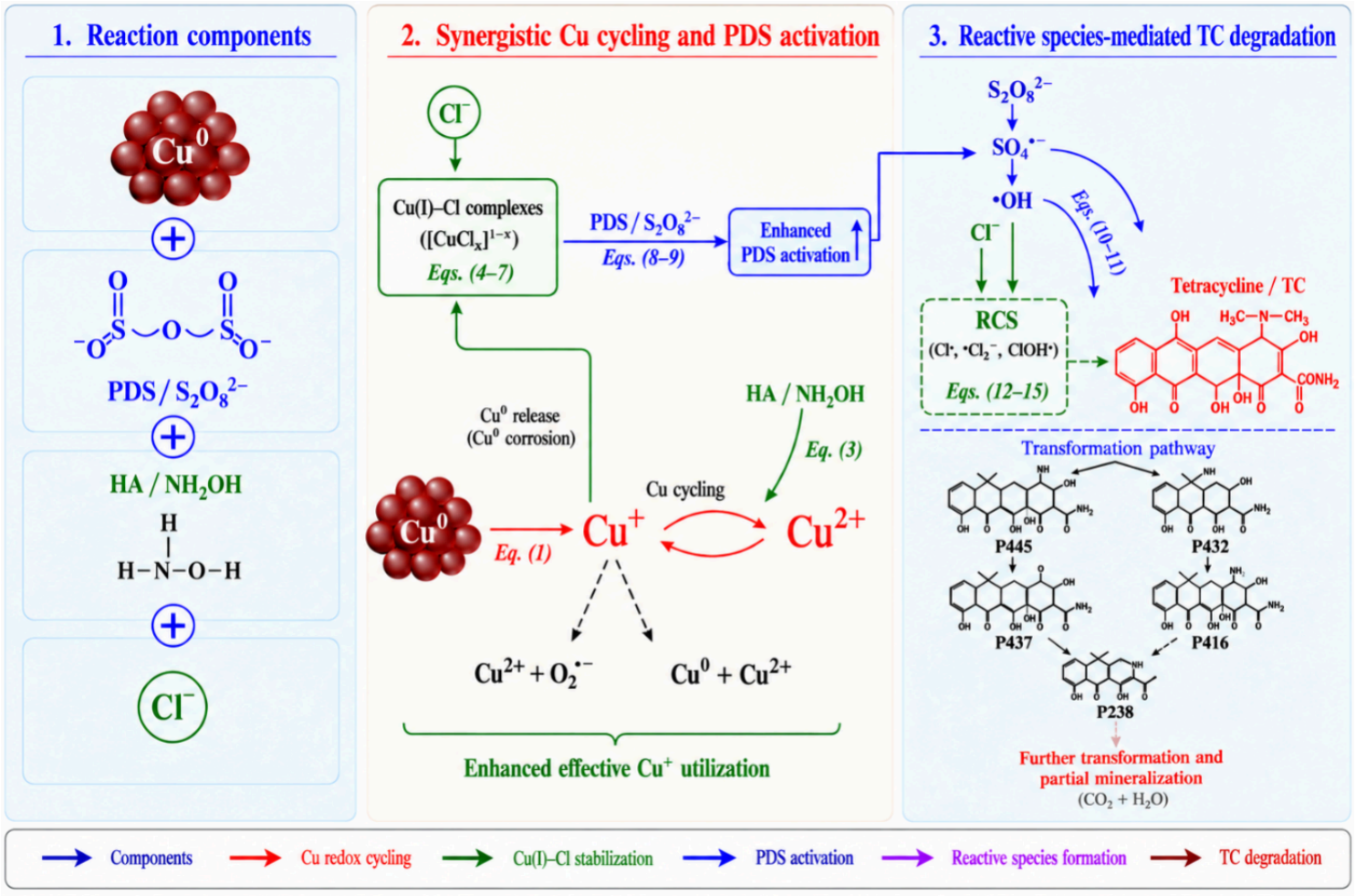


Figure 6

Reaction mechanism of HA/Cl^--enhanced Cu^0/PDS activation for tetracycline degradation. Reaction conditions: $[TC]_0$ = 5 mg/L, $[Cu^0]_0$ = 0.05 g/L, $[HA]_0$ = 0.3 mmol/L, $[PDS]_0$ = 0.1 mmol/L, $[Cl^-]_0$ = 3 mmol/L, pH = 5.0 ± 0.1, T = 25 ± 1 °C

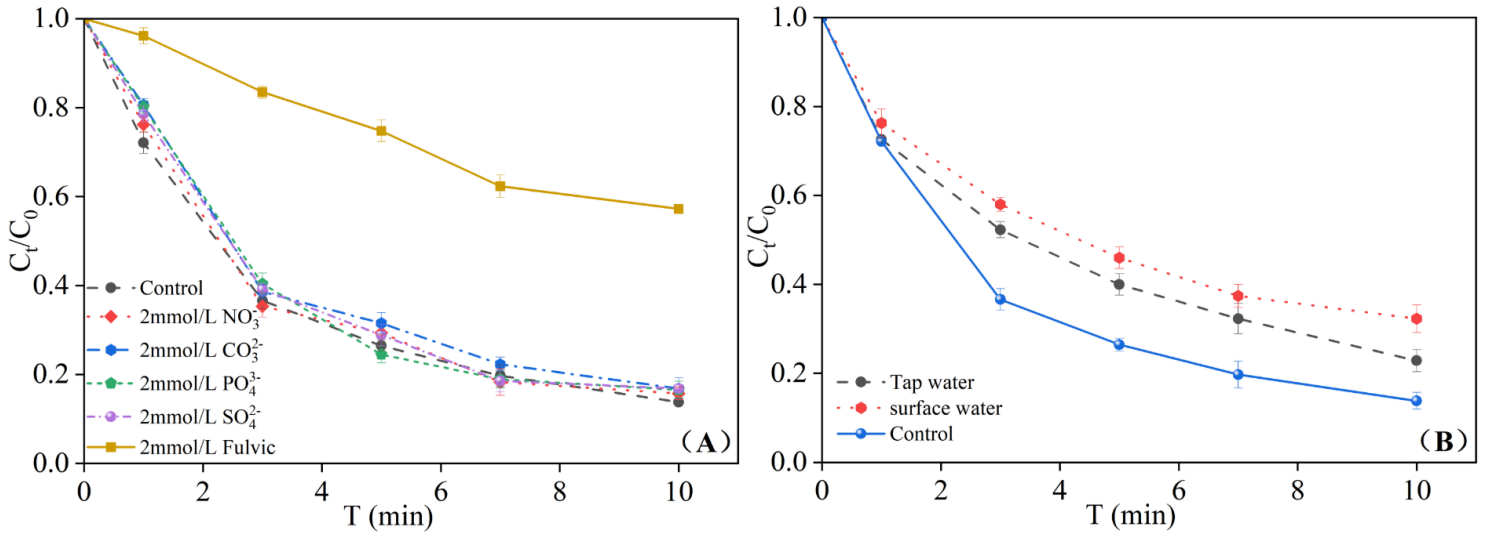


Figure 7

Effects of water matrix components on TC degradation in the Cu^0/PDS/HA/Cl^- system (A), and degradation performance of TC in two real water samples, namely tap water and surface water (B). Reaction conditions: $[TC]_0$ = 5 mg/L, $[Cu^0]_0$ = 0.05 g/L, $[HA]_0$ = 0.3 mmol/L, $[PDS]_0$ = 0.1 mmol/L, $[Cl^-]_0$ = 3 mmol/L, pH = 5.0 ± 0.1, T = 25 ± 1 °C

Supplementary Files

This is a list of supplementary files associated with this preprint. Click to download.

- 02Supplementarymaterials.docx
- 04Graphicalabstract.docx